Waste Heat-Based Thermal Corer for Lunar Ice Extraction

Kuan-Lin Lee[1], Quang Truong[1], Sai Kiran Hota[1], Srujan Rokkam[1]
[1] *Advanced Cooling Technologies, Inc., Lancaster, PA, 17601*

Kris Zacny[2]
[2] *Honeybee Robotics, Altadena, CA, 91001*

The water ice accumulated in the Permanently Shadow Regions (PSR) of the Moon is considered to be the most valuable resource on the moon since it can be processed to generate Oxygen for life-supporting and converted into LH2 and LO2 for satellite and spacecraft refueling. It has been demonstrated that water can be extracted from icy-soil through in-situ heating and then collected by re-freezing the sublimated vapor within a cold trap container. Under this research, a thermal management system (TMS) for Lunar Ice Miners was developed, which consists of a thermal corer that can strategically use the waste heat of on-board nuclear power sources for ice extraction, and a cold trap tank than can use the lunar cold environment as the heat sink for ice collection. In order to investigate heat exchange between the corer and icy-regolith during the thermal extraction process, a two-dimensional transient model was developed and built-in ANSYS FLUENT environment as user-defined functions (UDF). The UDF provides the user-defined material properties of the icy-regolith as a function of temperature and porosity, including specific heat, thermal conductivity, saturation pressure, and mass fraction of ice.

Nomenclature

ACT	=	Advanced Cooling Technologies, Inc.
HBR	=	HoneyBee Robotics
MMRTGs	=	Multi-Mission Radioisotope Thermoelectric Generators
TMS	=	Thermal Management System
ID	=	Inside Diameter
$w_{Regolith}$	=	Mass Fraction of Regolith
w_{ice}	=	Mass Fraction of Ice
C_P	=	Specific Heat
dt	=	Time Step
T	=	Temperature
L_s	=	Latent Heat of Sublimation of Ice
k	=	Thermal Conductivity
v	=	Porosity
M_w	=	Molecular Weight
$\hat{R}$	=	Ideal Gas Constant
P_{sat}	=	Saturation Pressure

I. Introduction

IN 2009, the Lunar CRater Observation and Sensing Satellite (LCROSS) mission confirmed the existence of water ice in the craters of the polar regions on the moon. Based on their data, the concentration of water ice mixed with the dry regolith was estimated to be ~5.6%wt [1]. The long-term goal of Lunar In-situ Resource Utilization (ISRU) is to mine water from the polar crate in a rate of 15 metric tons per year [2]. It has been demonstrated that water can be extracted from icy-soil through in-situ heating and then collected by re-freezing the sublimated vapor within a cold trap container [3]. However, to warm up ice from a cryogenic temperature of 40K and sublimate it at 200K at a rate of 2.78 kg per hour, at least 2.3 kW of thermal energy will be needed. Inversely, around 2.2kW of thermal energy needs to be removed to refreeze and collect the sublimated vapor within the cold trap container. To meet this large thermal power requirement for ice mining, the most energy-economical solution is a Thermal Management System (TMS) for

Lunar Ice Miners, to utilize the waste heat of the two on-board Multi-Mission Radioisotope Thermoelectric Generators (MMRTGs) for extraction and using the extremely low environmental temperature (~40K) as the heat sink for ice refreezing within the cold trap tank, as shown in Figure 1. The TMS consists of the following components:

1. A mechanically pumped fluid loop (MPFL), which is a "thermal bus" to deliver and distribute the waste heat from an MMRTG to components that required thermal energy. The majority of the waste heat will be used for ice extraction.
2. Multiple waste heat-based coring drills (i.e. thermal corers) with embedded miniature flow channels. After the drill is inserted into the icy regolith, the heat delivered by the pumped loop will travel through the drills via mini-channels and directly warm up and sublimate the ice within the regolith.
3. A cold trap tank with integrated variable conductance heat pipes (VCHPs) that can switch between two modes of operation (ice collection and ice removal modes) without using any electricity and moving parts.
4. Rotary unions that couple the pumped fluid loop, thermal corer, and the cold trap.

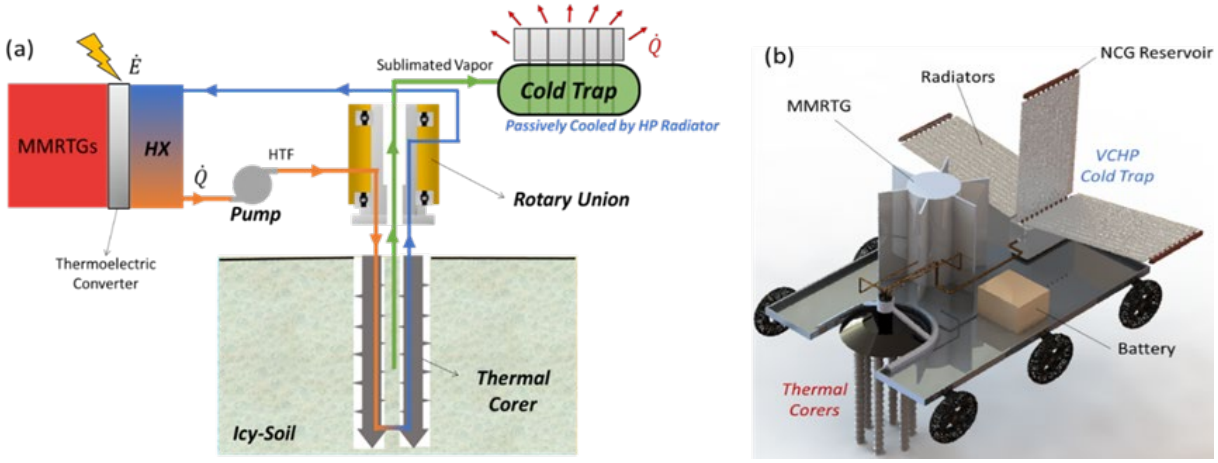

Figure 1. The thermal management system for Lunar Ice Miners, consisting of a pumped fluid loop, a waste heat-based thermal corer, rotary unions and a passively cooled VCHP cold trap (a) system diagram (b) render model showing a mining rover design.

In this work, a waste heat-based thermal corer was developed based on the coring drill design from Planetary Volatiles Extractor (PVEx). The thermal corer includes embedded mini-channels into the drill's wall, as shown in Figure 2. Two fluid passages are provided at the top of the thermal corer. The hot fluid passage is shown in red, and the cold outflowing fluid is shown in blue. The hot incoming fluid splits into 4 mini-channel passages near the top of the corer and flows downwards closer to the inner side of the corer. The size of the mini-channels for incoming fluid increases gradually, and the mini-channels eventually merge with the outflow channels at the bottom of the corer. This allows for more residence time of the hot fluid, so more heat is dissipated for sublimation. The hot fluid temperature decreases as ice is sublimated and the cold fluid then flows outside of the thermal corer at the top. The outflowing cold fluid passage is along the other annual space closer to the outside wall of the corer.

To investigate heat and mass transfer aspects during a thermal extraction process, a 2D transient FEA-based thermal model was developed through ANSYS Fluent. Thermo-physical properties of ice and regolith such as thermal conductivity, specific heat, latent heat, vapor pressure, etc. were specified by User Defined Functions (UDF).

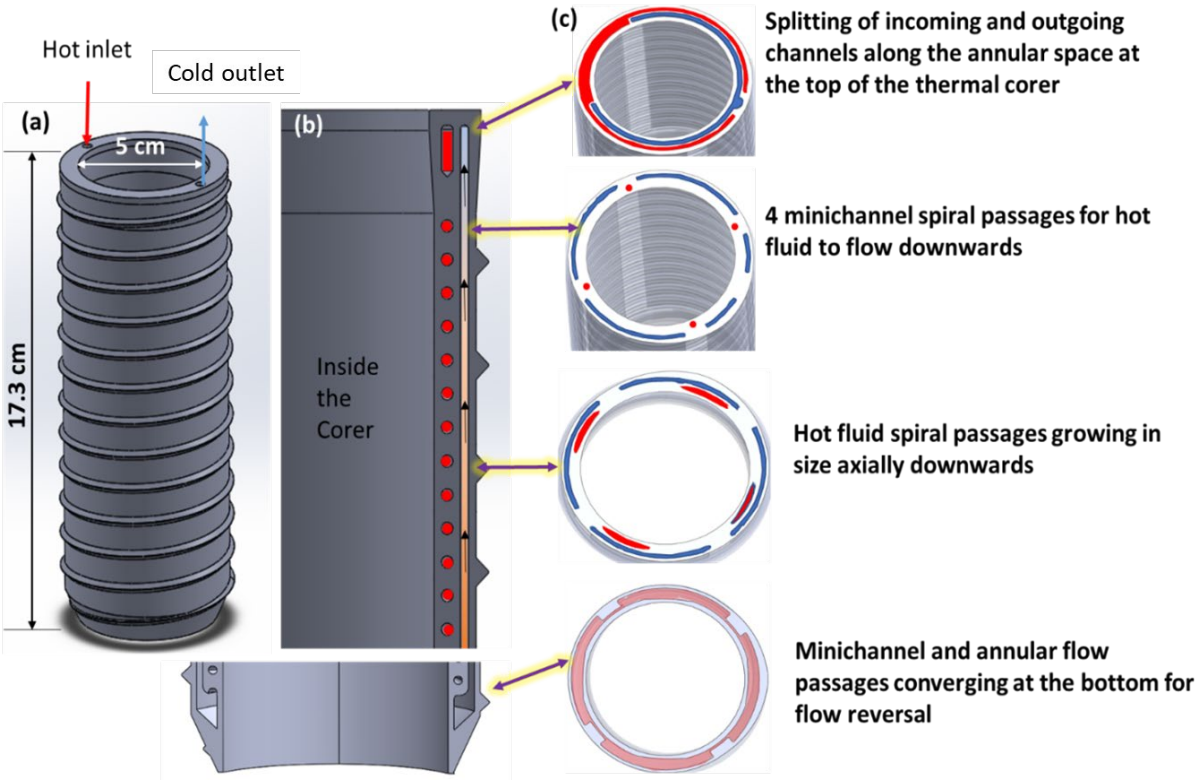

Figure 2. (a) 3D CAD model of the thermal drill corer, (b) internal geometry of the corer showing fluid passage (c) Cross-sectional view of how fluid flowing into the thermal corer through mini-channels, and annual flow return.

II. Model Development for Thermal Extraction Process

The thermal properties of the icy-regolith are based on previous works from Metzger et al [4], and Feistel et al [5]. As shown in Figure 3, the thermal conductivity of icy-regolith is a function of porosity, pressure, and temperature, which can vary widely from 10^{-3} to 1 W/m·K. The correlation for thermal conductivity of icy-regolith is shown in Eq. (1):

$$k(T,P,\nu) = -k_1 e^{(-k_4\nu)}(1-k_5T^3) + k_6\hat{P}^{(k_2-k_3\nu)}e^{\left(-k_7\nu+(k_8\nu-k_9)Ln^2\hat{P}\right)} \quad (1)$$

The coefficients used in this correlation are listed in Table 1. In this work, the porosity (ν) was selected to have a constant value of 0.3.

Table 1. Coefficients for Eq. 1

$\hat{P}$	P_0	k_1	k_2	k_3	k_4
max (P_{sat}, P_0)	13.6850862	3.419684	1.340911	0.680958	2.854397
k_5	k_6	k_7	k_8	k_9	
3.70E-08	0.79908959	2.637143	0.024344	0.047937	

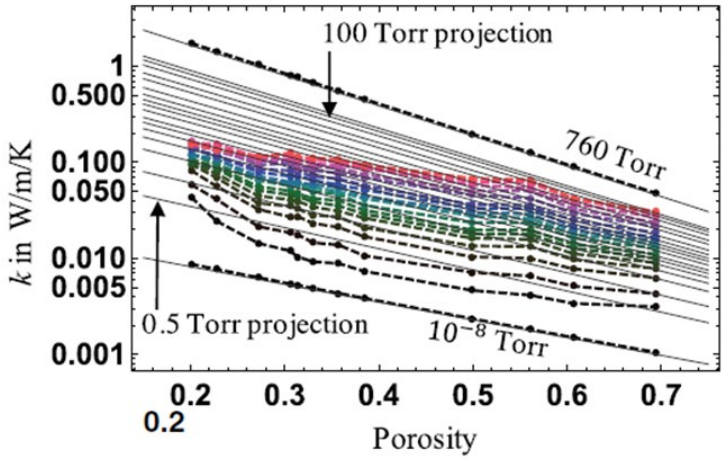

Figure 3. Thermal conductivity of icy-regolith comparison between a correlation model (gray lines) with test data set (color lines) [4].

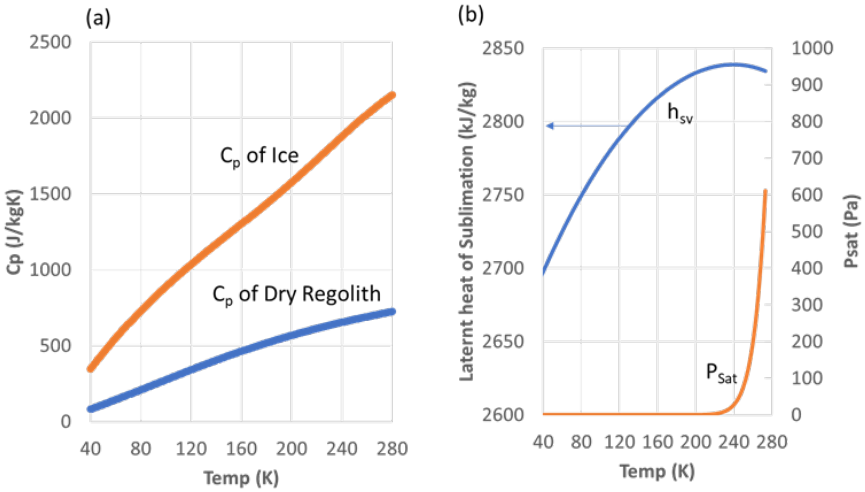

Figure 4. (a) Specific heat of ice and dry regolith (b) latent heat and saturation pressure of water from a temperature range of 40K to 280K.

Figure 4 shows the specific heat values of ice and dry regolith. Before phase transition happens, the specific heat of icy-regolith is a function of specific heat and mass fraction of dry regolith and ice. During sublimation, the specific heat of icy-regolith becomes a function of latent heat. The equation for specific heat of icy-regolith is shown in Eq. (2):

$$C_P(T) = w_{Regolith} C_{P_{Regolith}} + w_{ice} C_{P_{ice}} \tag{2}$$

Where:

$$C_{P_{Regolith}}(T) = -23.173 + 2.127T + 0.015T^2 - 7.3699 \times 10^{-5}T^3 + 9.6552 \cdot 10^{-8}T^4 \tag{3}$$

$$C_{P_{ice}}(T) = -100.5 + 11.43T + 7.101 \cdot 10^{-3}T^2 - 3.987 \cdot 10^{-4}T^3 + 2.075 \cdot 10^{-6}T^4 - 3.2 \cdot 10^{-9}T^5 \tag{4}$$

$w_{Regolith}$ and w_{ice} are the mass fraction of regolith and ice. During sublimation, the specific heat of icy-regolith is dominated by the latent heat of sublimation. To simulate this process, an artificial specific heat $\widehat{C_P}$ is introduced, which can be described in Eq. (5):

$$\widehat{C_P}(T) = w_{ice}\frac{L_s}{\Delta T} \tag{5}$$

Where $\boldsymbol{L_s}$ is the latent heat of sublimation of ice, which is assumed to be constant at 2,800 kJ/kg. ΔT is the temperature window of phase transition, typically less than 5 K. For example, with a 5% initial mass fraction of ice and $\Delta T = 2$ K, Eq. (5) gives a value of specific heat of 70 kJ/kg·K. The sublimation is triggered by a decrease in initial mass fraction of ice of each calculation cell, and stopped when the mass fraction of ice reaches 0 value.

In order to calculate thermal conductivity and specific heat above, the saturation pressure of sublimated ice and mass fraction of the ice in the icy-regolith need to be calculated. The equations for saturation pressure and water vapor generation are:

$$P_{sat}(T) = 14050.7T^{3.53}exp\left(-\frac{5723.265}{T} - 0.00728332T\right) \tag{6}$$

$$m_v(t+dt) = m_v(t) + [P_{sat}(T(t)) - P(t)] \times \sqrt{\left(\frac{M_w}{2\pi\hat{R}T(t)}\right)} \times dt \times A_{core} \tag{7}$$

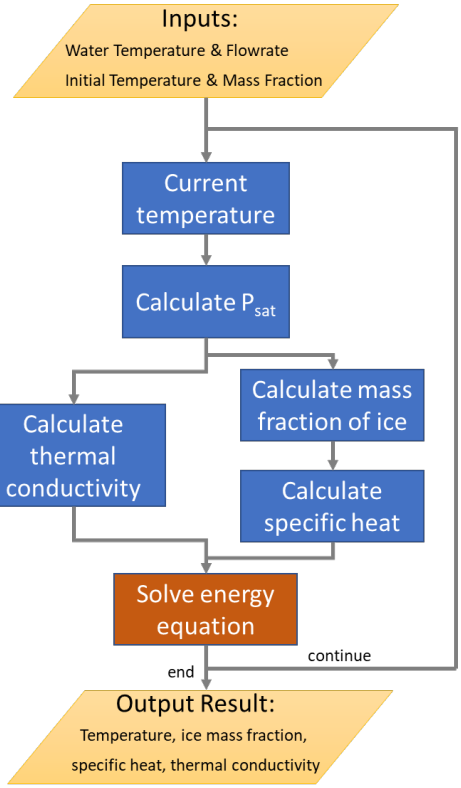

Figure 5. Schematic of FLUENT's solver with UDFs. Based on current temperature, Psat will be calculated and used to obtain conductivity, mass fraction of ice, and specific heat. Then, energy equation will be solved using the new thermal properties to obtain the new temperature in the next time step.

The equations above were implemented into ANSYS-FLUENT as a user defined function (UDF) to provide the user-defined material properties of the icy-regolith, including: specific heat, thermal conductivity, saturation pressure,

and mass fraction of ice. During simulation, FLUENT will use the equations in UDFs to calculate icy-soil properties based on current temperature, and use those properties to solve energy equation to update temperature for the next time step. The schematic of FLUENT solver with UDFs is shown in Figure 5.

In the previous work [6], a preliminary model was validated against experimental water extraction of Mars regolith and Lunar regolith. Both experiment and simulation demonstrated a complete sublimation 10% wt of icy-soil within ~ 9 minutes, using a thermal corer with 6 inches in length, 0.6 inches in inside diameter, and wall temperature of 57 °C. On-going work focuses on optimizing the dimension of the full-scale corer, using the developed model, to achieve the targeted water collection of 2.78 kg/hr. Further improvement to the model was made to include conjugate heat transfer between hot fluid and the corer.

III. Thermal Corer Prototype Fabrication and Test Setup

To demonstrate the feasibility of fabrication, ACT designed and fabricated a reduced-scale thermal corer via additive manufacturing. The corer will be used for experimental testing and validation of the thermal model. The dimensions of the corer are shown in Table 2.

Table 2. Specification of the 3D-printed thermal corer

Specification	Dimension (mm)
Corer's Length	172.72
Corer's Inside Diameter	50
Mini-channel's Inside Diameter	1.5
Mini-channel's Pitch	16.5
Mini-channel's Number	4

The thermal corer was 3D printed in stainless steel 316 (SS-316), according to the dimensions mentioned in Table 2. Figure 6 shows the photographs of the 3D printed thermal corer with embedded mini-channels. The spiral mini-channel inside the wall material can be seen from the radiography image shown in Figure 6(c). After welding the fluid transport lines (two HTF lines and, one volatile line), the thermal corer was ready for testing.

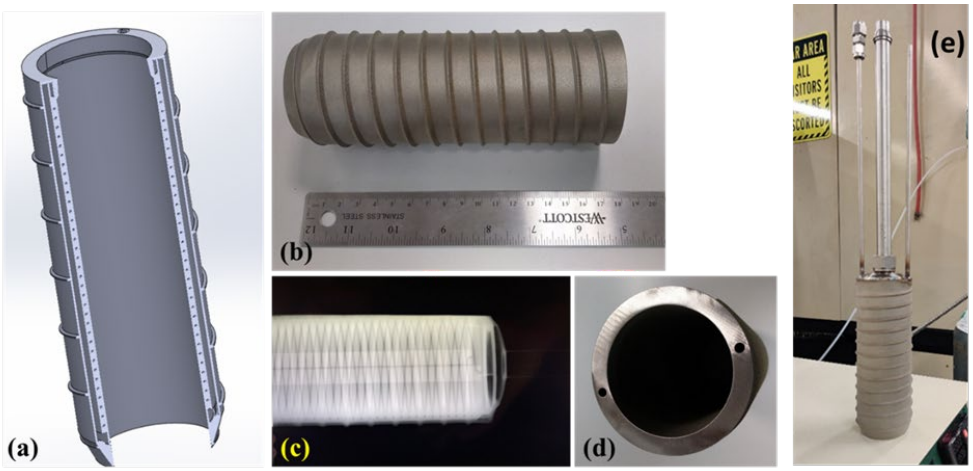

Figure 6. 3D-printed thermal corer: (a) cut-view model, (b) side-view of the actual printed part, (c) x-ray & leak-check were performed, (d) top-view of thermal corer, (e) Welded liquid line on the thermal corer.

A test setup for thermal corer performance characterization and CFD validation is being constructed at ACT. Figure 7 shows the CAD model of the test setup being constructed.

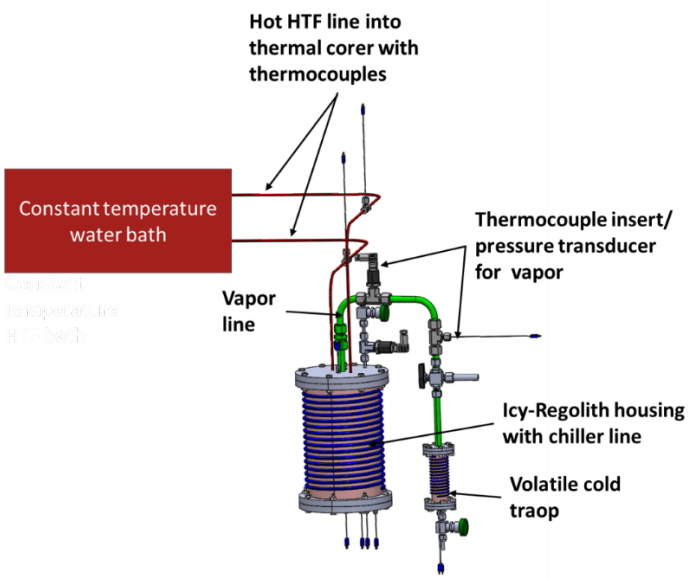

Figure 7. CAD model showing test components for thermal corer performance testing for ice-extraction.

The thermal corer will be placed in the regolith housing, and the rest of the space will be filled with regolith (5% wt ice). The HTF from the constant temperature water bath will flow through the thermal corer mini-channels and sublimate ice from the regolith. A vapor line is provided for the volatile (water vapor) and eventually to be collected in the volatile cold trap. The volatile cold trap in this testing will be a simple vessel with LN cooling coil wrapped around the cold trap. A pressure transducer will be used to monitor the pressure in the regolith housing and the vapor flow. The numerical code being developed will use this vapor pressure as the back-pressure in future calculations. Thermocouples will be placed strategically to record the temperature variation within the regolith housing and inside the thermal corer, as shown in Figure 8. The thermocouples inside the thermal corer will be placed at the center, mid-distance from the wall and near the wall. These temperatures, and the ice extraction rate will be used to validate the numerical model. Additionally, another thermocouple will be inserted in the volatile cold trap to record the condensing volatile temperature. Filters to avoid sand flowing into the volatile cold trap will be placed in the vapor lines. Before the start of each test, the whole system will be vacuumed to relevant pressures (<0.001 Torr) by means of attaching a vacuum pump to the vacuum valve.

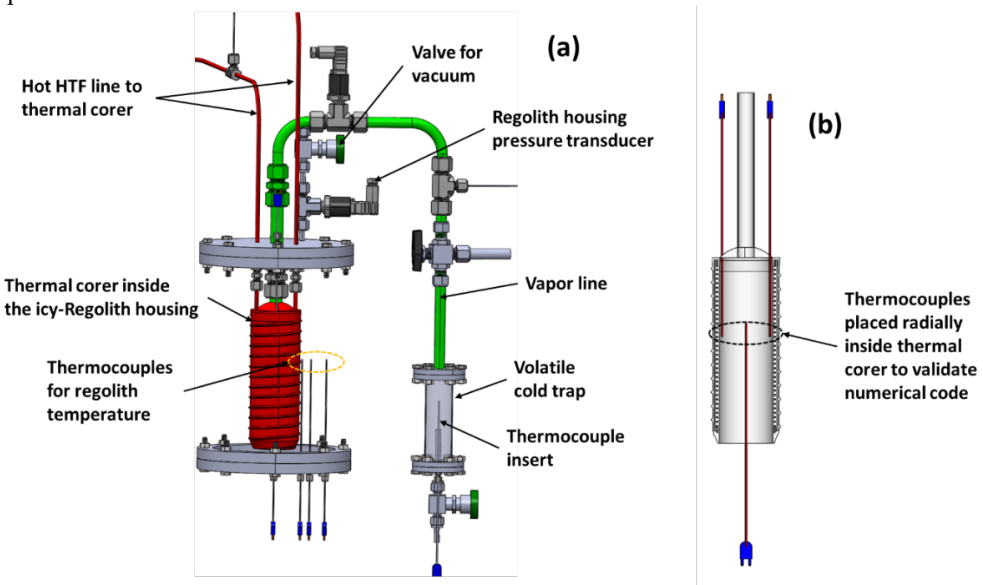

Figure 8. Temperature and other measurement devices in the regolith housing and other components to record operating parameters during testing.

The entire system is being constructed from off-the-shelf stainless steel 316 components. ACT has fabricated the regolith housing and the volatile cold trap as shown in Figure 9. The top and bottom of the cylinders have a flange connection via a gasket to ensure proper vacuum. This allows for easy removal of the icy regolith in between experiments. Copper tubes will be wrapped along the length of these components for LN2 cooling to maintain desired operating temperatures (lunar). After assembly of the components, blanked heaters and insulation will be wrapped around the vapor (volatile) line to avoid condensation.

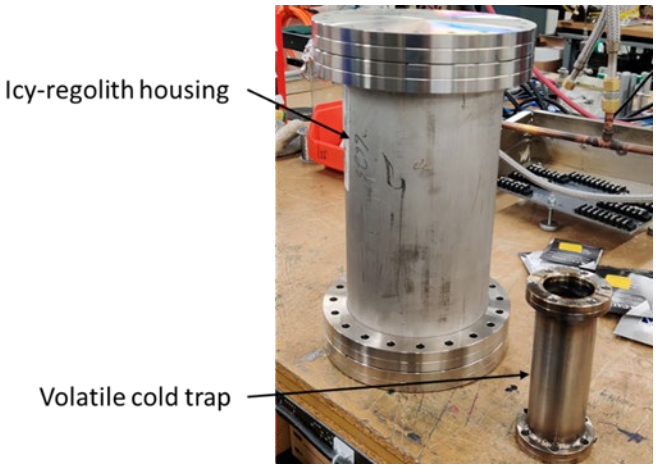

Figure 9. Icy-regolith housing and volatile cold trap that will be used for thermal corer performance testing.

IV. Analysis and Optimization of Waste Heat-Based Thermal Corer

A. Thermal Corer Structural Analysis

The structural analysis was performed on the 3D-printed corer, and an equivalent standard corer without mini-channel, as shown in Figure 10. The material properties of SS-316 were used in this analysis. The drilling conditions were: 10 N·m in torque, 100 N in vertical force.

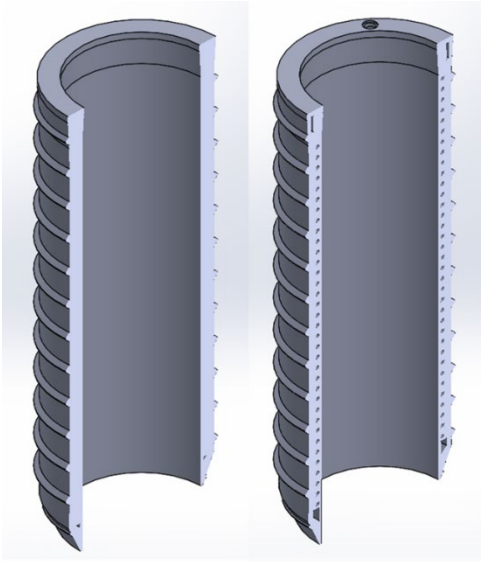

Figure 10. (a) Standard corer without mini-channels, (b) ACT's corer with 4 mini-channels. The material properties are of SS-316. The drilling conditions were 10 N·m in torque and 100 N in vertical force.

The structural analysis was performed in ABAQUS Standard. Figure 11 shows the Von Mises stresses of ACT's 4-channel corer, versus standard corer. The standard corer without any mini-channels experienced high stresses near the tip, in which the highest value was 5.73 MPa. On the other hand, ACT's 4-channel corer also experienced high stresses near the tip, but with a slightly higher stress value of 8.58 MPa. Based on the yield strength of SS-316 at 200 MPa, the safety factors are all above 23. Under standard drilling conditions of 10 N·m in torque and 100 N in vertical force, ACT's printed 4-channel corer is structurally stable.

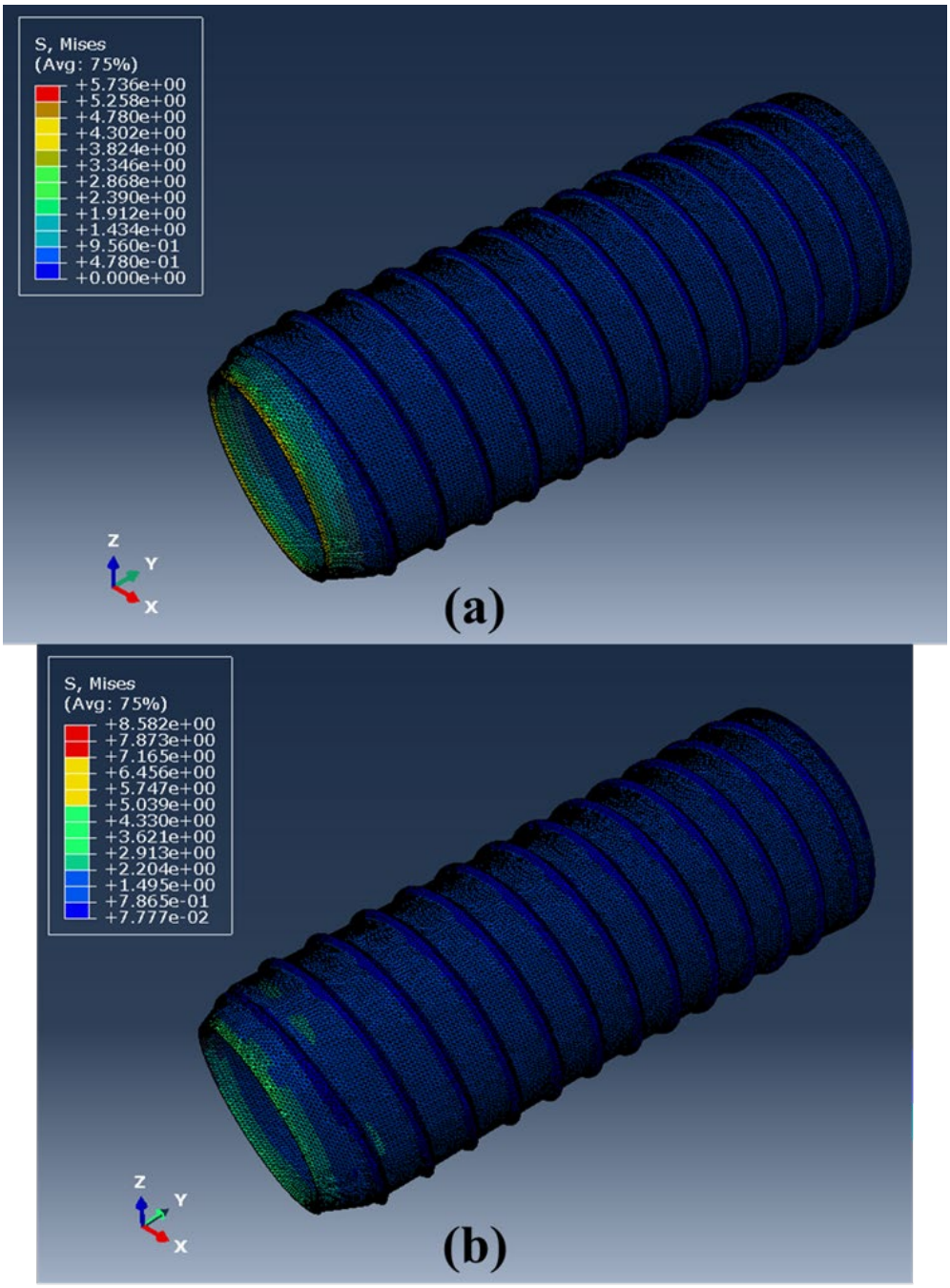

Figure 11. Structural analysis using ABAQUS: (a) Standard corer without mini-channels, (b) ACT's corer with 4 mini-channels.

B. Thermal Model Improvement with Conjugate Heat Transfer

To improve the thermal model to accurately capture the heat transfer and extraction process, the heat source was modeled based on conjugate heat transfer from hot water liquid transferring to the solid corer, and from the corer to icy-regolith. Thus, the boundary condition inputs became the hot water's temperature and flow rate, instead of simply uniform wall temperature. Figure 12 shows the direction of the hot water, looping from top left to the top right of the corer. The simulation domain is a symmetry domain to reduce computational time. In this model, the corer was assumed to be already inserted into the icy regolith, because the focus was to simulate and to verify sublimation of ice inside the regolith. After the numerical model is validated with the experiment, sublimation during drilling (different temperature) can be further analyzed.

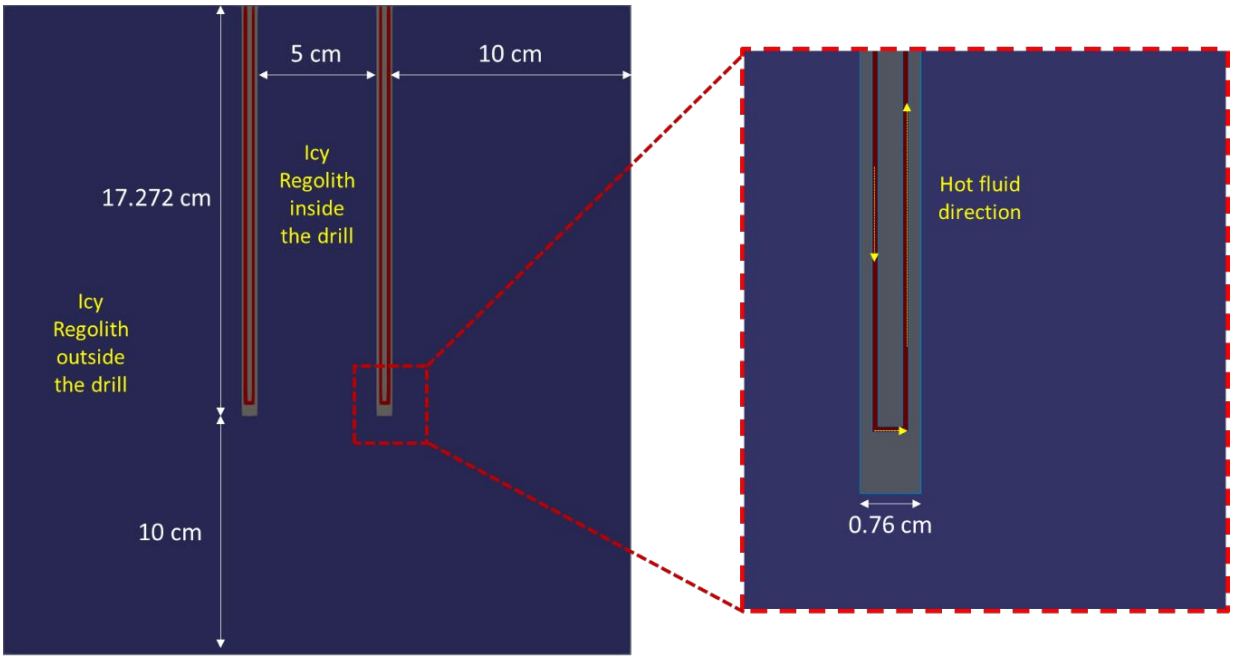

Figure 12. Symmetry domain of the full-length drill in icy-regolith environment. The corer is in gray color (50 cm in length, 5 cm in inside diameter, 0.76 cm in thickness). The ice is in blue color. The heat transfer fluid is in red color. The arrows show the fluid direction, from top left to top right, to provide heat to the corer.

The thermal corer shown in Figure 12 was simulated with hot water's flow rate inside the mini-channels of 3.38 cc/s, hot water's temperature of 50 ℃, ambient temperature of -50 ℃, and initial ice mass fraction of 5%. Figure 13 and Figure 14 show the temperature profile and mass fraction of ice at 3 seconds and 1037 seconds. At time = 3 s, the hot water (50 ℃) started to go downward from the inside of the corer, then looped upward to the outside of the corer, causing an increase in temperature via conduction. At time = 1037 s, Temperature increased inside the corer, causing sublimation of approximately 30% of the ice inside. On-going work at ACT is to verify and validate the thermal model with conjugate heat transfer through experimental testing.

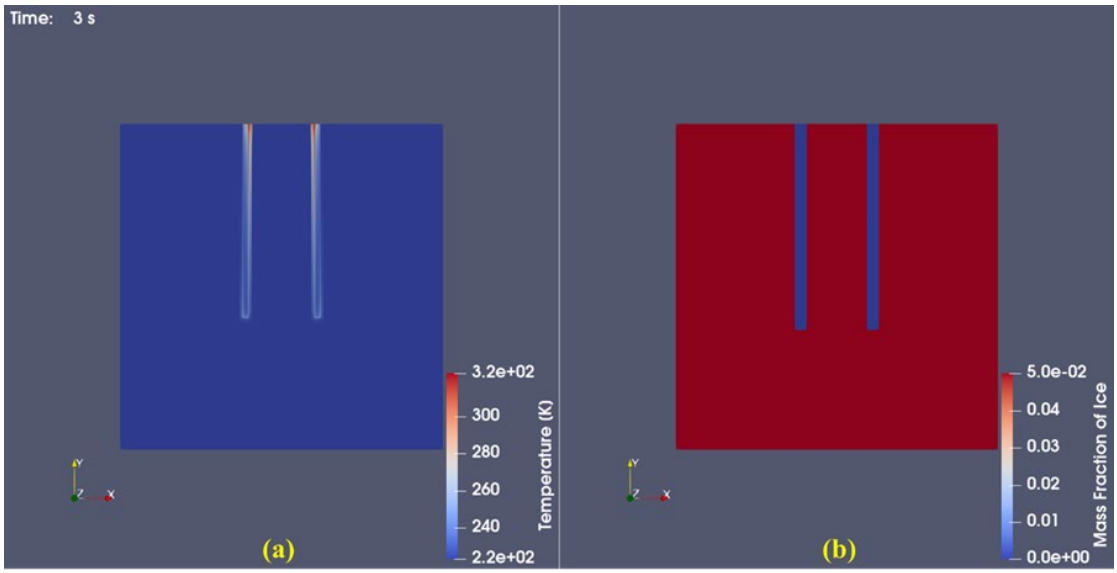

Figure 13. CFD simulation of validation case (L=17.272 cm, ID=5 cm), at time = 3s: (a) temperature profile, (b) mass fraction of ice. The hot water (3.38 cc/s, 50 °C) started to go downward from the inside of the corer, then looped upward to the outside of the corer, then looped upward to the outside of the corer, causing an increase in temperature via conduction.

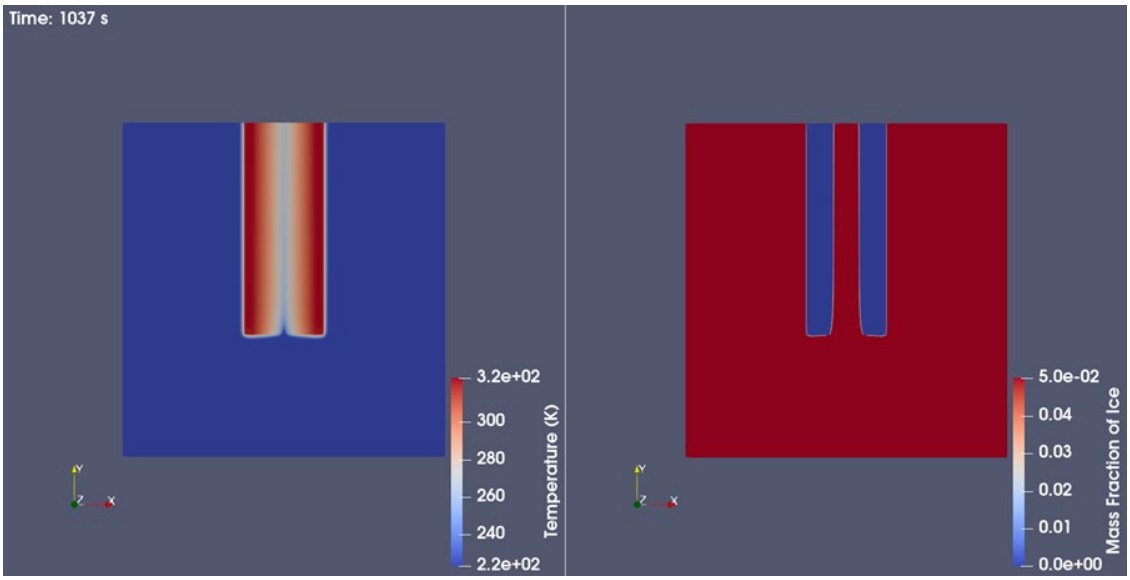

Figure 14. CFD simulation of validation case (L=17.272 cm, ID=5 cm), at time = 1037s: (a) temperature profile, (b) mass fraction of ice. Temperature increased inside the corer, causing sublimation.

Three point-locations inside the corer's domain were extracted to compare the temperature profiles, as shown in Figure 15. Point #1 closest to the corer's wall increased temperature first, followed by point #2 at quarter, and point #3 near the corer's center. During phase change, the temperature remained unchanged for a short period of time, which is shown more visibly on point #1 temperature profile.

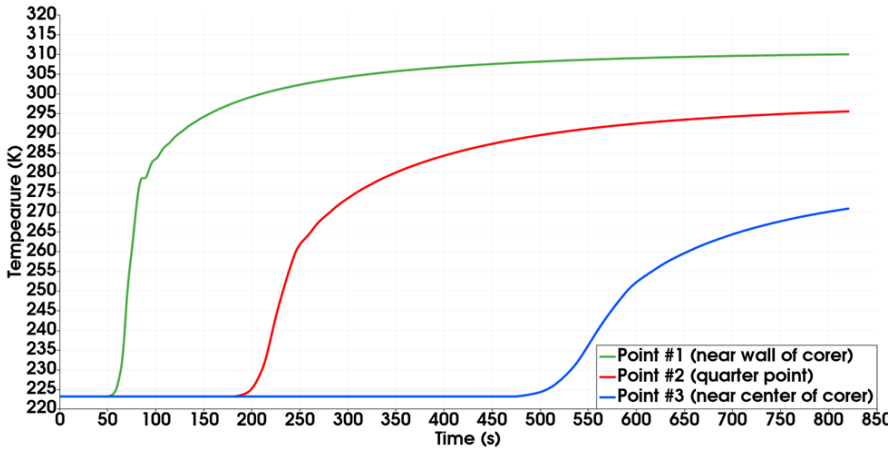

Figure 15. Temperature profile of three selected points inside the corer. Point #1 closest to the corer's wall increased temperature first, followed by point #2 at quarter, and point #3 near the corer's center. During phase change, the temperature remained unchanged for a short period of time, which is shown more visibly on point #1 temperature profile.

C. Parametric Sensitivity Study

The parametric sensitivity study was performed to further verify the thermal model as well as investigate the effects of hot fluid's flow rates, pumping powers, and back pressures (collection tank pressure). The flow rate of hot fluid has a large influence on the extraction rate due to heat transfer. However, increasing the flow rate will increase the pumping power, which is limited on an MMRTG. The parametric study on fluid flow rates will determine the most efficient pumping power for ice mining. The back pressure is another parameter that influences the performance of the thermal corer. Based on Eq. (7), the water vapor generation rate depends on the difference between saturation pressure and back pressure. Therefore, the cold trap in a vacuum condition will provide the highest extraction rate, and increasing back pressure will decrease the extraction rate.

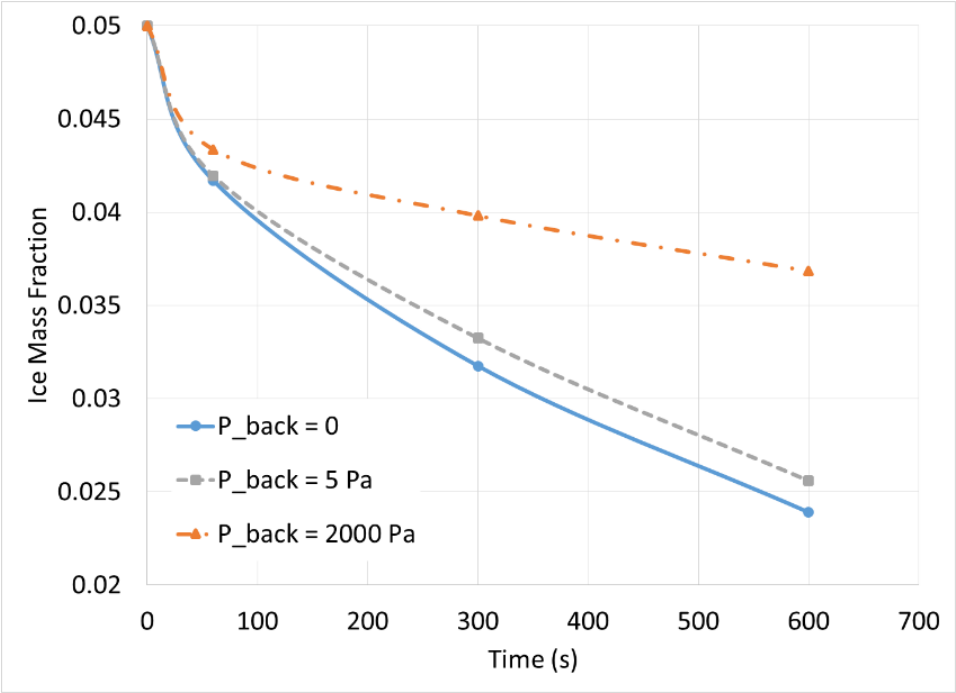

Figure 16. Mass fraction of ice inside the corer during extraction. The initial mass fraction is 5%. The back pressure (P_back) was set at vacuum, 5 Pa, and 2000 Pa. With higher back pressure, the ice extraction is slower.

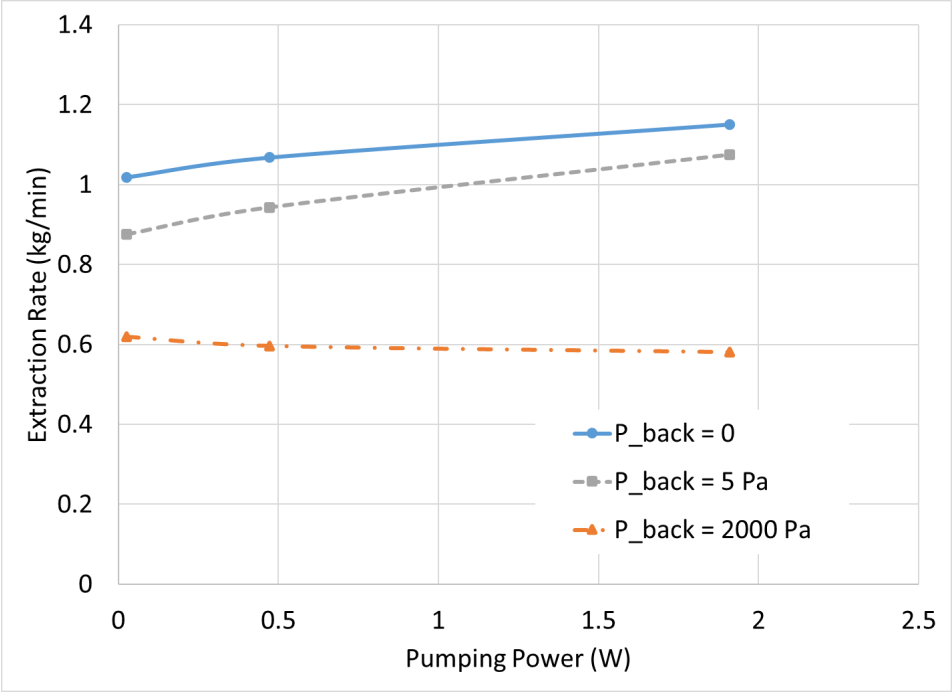

Figure 17. Ice extraction rates under different back pressures. The highest extraction rate is under vacuum. Under extremely high back pressure of 2000 Pa, the extraction rate decreased to a constant minimum.

In this study, the initial mass fraction of ice inside the regolith is 5%. Figure 16 shows the mass fraction of ice inside the thermal corer during extraction. The back pressure values were 0 Pa, 5 Pa, and 2000 Pa. The zero value represents vacuum condition, while the value of 5 Pa represents saturation pressure at -50 ℃, and the value of 2000 Pa represents a high-pressure condition corresponding to saturation water temperature of 20C. As a result, the ice extraction is slower under higher back pressure. Figure 17 shows the effect of back pressure on ice extraction rate. As expected, the highest extraction rate is under vacuum, and the extraction rate reduced under higher back pressure. Under 2000 Pa, the extraction rate experienced a minimum constant of 0.6 kg/min regardless of increasing the flow rate of HTF. The reduction of ice extraction is due to reduction of vaporization rate as shown in Equation (7). In real application, back pressure value will not stay as a constant. It will depend on the cooling boundary condition applied to the cold trap tank. This part of analysis is still undergoing.

Figure 18 shows the effect of hot fluid flow rate on extraction time. In this study, the back pressure was set a vacuum. Three different flow rates were investigated, including; 3.38 cc/s, 10.14 cc/s, and 17 cc/s. Inlet fluid temperature is 50C for three cases. As expected, a higher flow rate of hot fluid going through the mini-channels reduced the extraction time. As a result, a higher flow rate of the hot fluid reduces the time for ice extraction. However, increasing the flow rate significantly increases the pumping power, as shown in Figure 19.

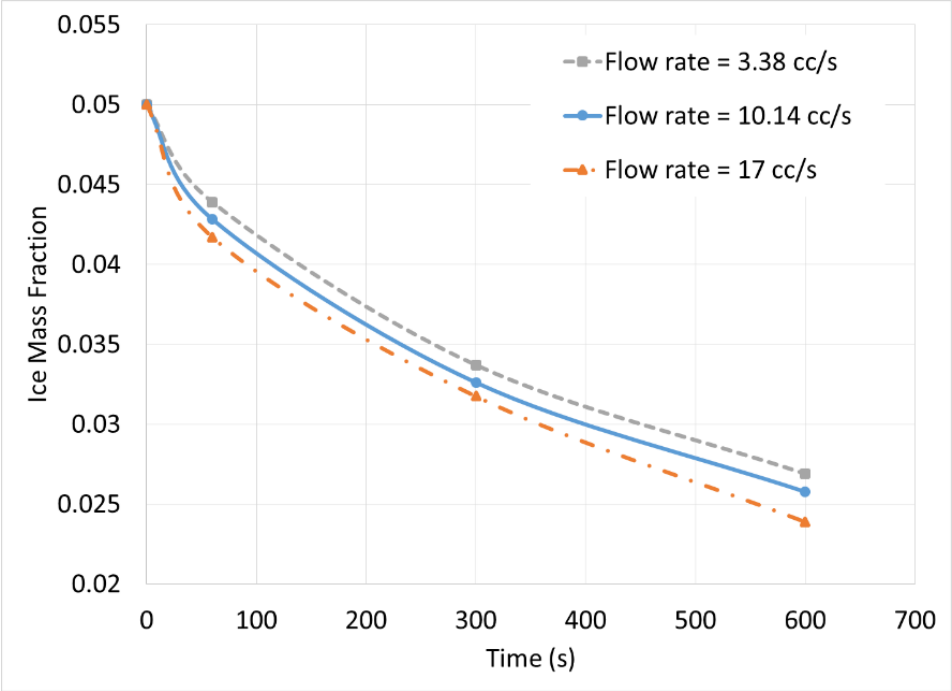

Figure 18. Mass fraction of ice inside the corer during extraction. The initial mass fraction is 5%. The back pressure (P_back) was set at vacuum. The hot water flow rate was set at 3.38, 10.14, and 17 cc/s. Higher flow rate increased the extraction rate.

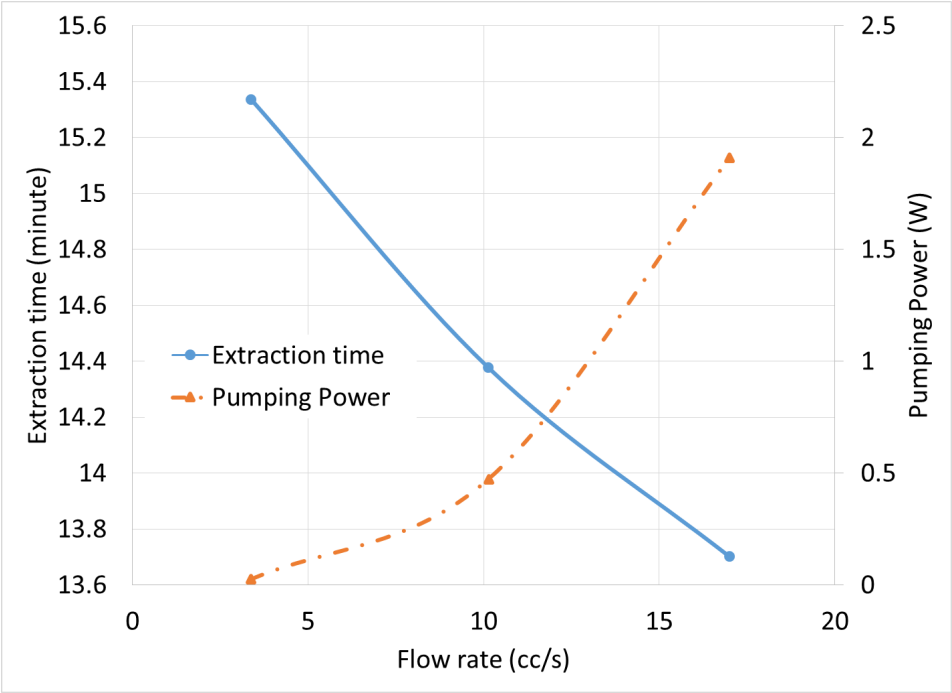

Figure 19. Mass fraction of ice inside the corer at different flow rates and pumping powers. The back pressure was set at vacuum. Increasing the flow rate significantly increases the pumping power, but reduces the extraction time.

V. Conclusion

In this research, a preliminary design of the waste heat-based thermal corer was developed with a more representative inside diameter of 5 cm, and length of 17 cm. Internally, two fluid passages are provided at the top of the corer, splitting into 4 mini-channels and spiraling downwards closer to the inner side of the corer. The corer design was confirmed structurally stable, under standard drilling conditions of 10 N·m in torque and 100 N in vertical force. Subsequently, the thermal corer was 3D printed in stainless steel 316 and will be used for experimental testing and validation of the thermal model.

The model for the waste heat-based thermal corer was developed and implemented into ANSYS-FLUENT as a user-defined function (UDF) to provide the user-defined material properties of the icy-regolith. The model uses heat source from conjugate heat transfer from hot water liquid transferring to the solid corer, and from the corer to icy-regolith. Thus, the boundary condition inputs are the hot water's temperature and flow rate instead of artificial wall temperature. The sublimation simulation was performed using the 2D equivalence of the 3D-printed corer. If the hot water's flow rate inside the mini-channels is 3.38 cc/s, hot water's temperature is 50 ℃, and ambient temperature is -50 ℃; sublimation of approximately 30% of the ice inside the corer occurred within 17 minutes.

Verification of the phase-change mechanism of the thermal model was performed by extracting the temperature profiles of three locations inside the corer at the same time frame. During phase change, the temperature remained unchanged for a short period of time. The parametric sensitivity study was performed with different flow rates, pumping powers, and back pressures. The modeling results were anticipated, where:

- The ice extraction is slower under higher back pressure and the highest extraction rate is under vacuum.
- A higher flow rate of hot fluid going through the mini-channels reduces the extraction time, thus, increasing the extraction rate. However, increasing the flow rate will also increase the pumping power.

The waste heat-based ice extraction technology described in the paper will enable future ice miners to directly use onboard heat sources for ice extraction, which can be MMRTGs (as the paper described) or electronics waste heat. Therefore, the electricity generated during the mission can be used for other purposes, such as powering the rover, driving the drill and pumping HTF. The modeling tools (thermal corer model, cold trap models) developed under this program will eventually lead to a system-level model that can help the designers to optimize drill configuration and rover arrangement to minimize electricity usage and maximize the extraction efficiency.

Acknowledgments

The research work in this paper was performed as a part of The National Aeronautics and Space Administration (NASA) Small Business Innovation Research (SBIR) Phase I (Contract: 80NSSC20C0339) and Phase II (Contract: 80NSSC21C0564) programs, awarded to Advanced Cooling Technologies, Inc. The authors would like to acknowledge the support and guidance provided by the technical monitor Naina Noorani from NASA Johnson Space Center.

References

[1] A. Colaprete, P. Schultz , J. Heldmann , D. Wooden, M. Shirley and K. Ennico, "Detection of Water in the LCROSS Ejecta Plume," Science, vol. 330, p. 463, 2010.

[2] G. Sanders, "NASA Lunar ISRU Strategy," 2019. [Online]. Available: https://ntrs.nasa.gov/archive/nasa/casi.ntrs.nasa.gov/20190032062.pdf.

[3] E. Ethridge and W. Kaukler, "Microwave Extraction of Water from Lunar Regolith Simulant," in Space Technology and Applications International Forum (STAIF-2007), 2007.

[4] P. T. Metzger, Z. Kris and M. Phillip , "Thermal Extraction of Volatiles from Lunar and Asteroid Regolith in Axisymmetric Crank-Nicolson Modeling," Journal of Aerospace Engineering , vol. 33, no. 6, 2020.

[5] R. Feistel and W. Wagner, "Sublimation pressure and sublimation enthalpy of H_2O ice between 0 and 273.16K," Geochimica et Cosmochimica Acta, vol. 71, pp. 36-45, 2007.

[6] Kuan-Lin Lee, Calin Tarau, Quang Truong, and Srujan Rokkam, "Thermal Management System for Lunar Ice Miners," 50th International Conference on Environmental Systems, July 2021.